Ore Geology Reviews 161 (2023) 105653

Contents lists available at ScienceDirect

Ore Geology Reviews

journal homepage: www.elsevier.com/locate/oregeorev

Big data analytics for mining geochemistry of gold mineralization: The Gandy gold deposit, the Toroud-Chah Shirin (TCS) belt, north Iran

Mahnaz Abedini [a], Mansour Ziaii [a], Timofey Timkin [b], Amin Beiranvand Pour [c,*]

[a] Faculty of Mining, Petroleum and Geophysics Engineering, Shahrood University of Technology, Iran
[b] School of Earth Sciences & Engineering, Tomsk Polytechnic University, 634050 Tomsk, Russia
[c] Institute of Oceanography and Environment (INOS), Universiti Malaysia Terengganu (UMT), 21030 Kuala Nerus, Terengganu, Malaysia

ARTICLE INFO

Keywords:
Big data analytics
Geoscience big data
Mining geochemistry
Mineralogical and geochemical type
Bayesian
Geochemical spectrum
Gandy gold deposit

ABSTRACT

Due to the complexity of the gold element, the mineralogical and geochemical investigations are significant to trace the gold behavior in sedimentary, metamorphic, magmatic, and post-magmatic processes and to identify the physicochemical conditions (i.e., pH, Eh, temperature, pressure) of concentration in the ore bodies. The trace elements may be concentrated as the primary or secondary haloes in endogenic and exogenic deposits with multi-formational types. Identification and separation of multi-formational geochemical halos associated with ore bodies have been the most significant challenge of gold deposits. Mining Geochemistry and Big Data analytics have become essential to identify the multi-formational geochemical anomalies for gold exploration in the Commonwealth of Independent States (CIS) countries. During the last three decades, pattern recognition techniques such as Bayesian and Geochemical spectra have been used to determine mineralogical and geochemical types of multi-formational anomalies. Big Data analytics has been used for integrating multi-type geoscience data and pattern recognition techniques to assess geochemical anomalies. In this study, Big Data analytics were used to generate the mineralogical and geochemical type (MGT) quantitative models based on the Bayesian, geochemical spectrum and hybrid methods for investigating the distribution of trace element contents of pyrite, galena, and sphalerite in the Gandy Gold Deposit, the Toroud-Chah Shirin (TCS) belt, north Iran. The multi-formational geochemical anomalies associated with gold mineralization in the Gandy deposit indicated a multi-MGT anomaly superposition, which is a combination of two MGTs: Au + Polymetals and Au + sulfide. The results of this study demonstrated a new perspective on the distribution of geochemical anomalies and the multi-MGT geochemical modeling for gold exploration in the TCS belt. Consequently, the instigated approach is greatly conceivable and applicable to reveal contrasting near-ore multi-formational geochemical haloes for gold exploration in many other metallogenic provinces.

1. Introduction

During the last three decades, Mining geochemistry methods have been applied to recognize geochemical anomalies related to blind mineralization (e.g., Grigorian, 1992; Ziaii et al., 2009a; Ziaii et al., 2012; Safari et al., 2016; Safari et al., 2018; Ziaii et al., 2019; Safari and Ziaii, 2019; 2020), to gold mineralization (Safonov, 1997; Ziaii et al., 1999; Grigorian et al., 1999a, 1999b; Veselovskii and Meshcheryakova, 2007; Ziaii et al., 2009b), and to mineral prospectivity mapping (MPM) (e.g., Ziaii et al., 2010; Ziaii et al., 2011; Timkin et al., 2022). Veselovskii and Meshcheryakova (2007) and Ziaii et al. (2009b) presented the structure of a data bank on the geology of mineral resources.

In recent years, Big Data (BD), given by Doug Laney (2001), has been the fourth scientific paradigm with the regular production of huge amounts of data. Hu, Wen, Chua and Li (2014) identified volume, generated rate, structure, data source, data integration, data store and access as the key factors which can discriminate between big data and traditional data. It has become a big challenge to process BD within an acceptable time and amount of resources. In order to efficiently extract value from BD, new methods are needed to process big data. For this reason, Big Data Analytics (BDA) has become a key factor to reveal hidden information and achieve competitive advantages (Philip, 2011; Chong and Shi, 2015). Big Data Analytics is an emerging field since massive storage and computing capabilities have been made available

* Corresponding author.
E-mail address: beiranvand.amin80@gmail.com (A.B. Pour).

https://doi.org/10.1016/j.oregeorev.2023.105653
Received 29 January 2023; Received in revised form 31 July 2023; Accepted 31 August 2023
Available online 3 September 2023

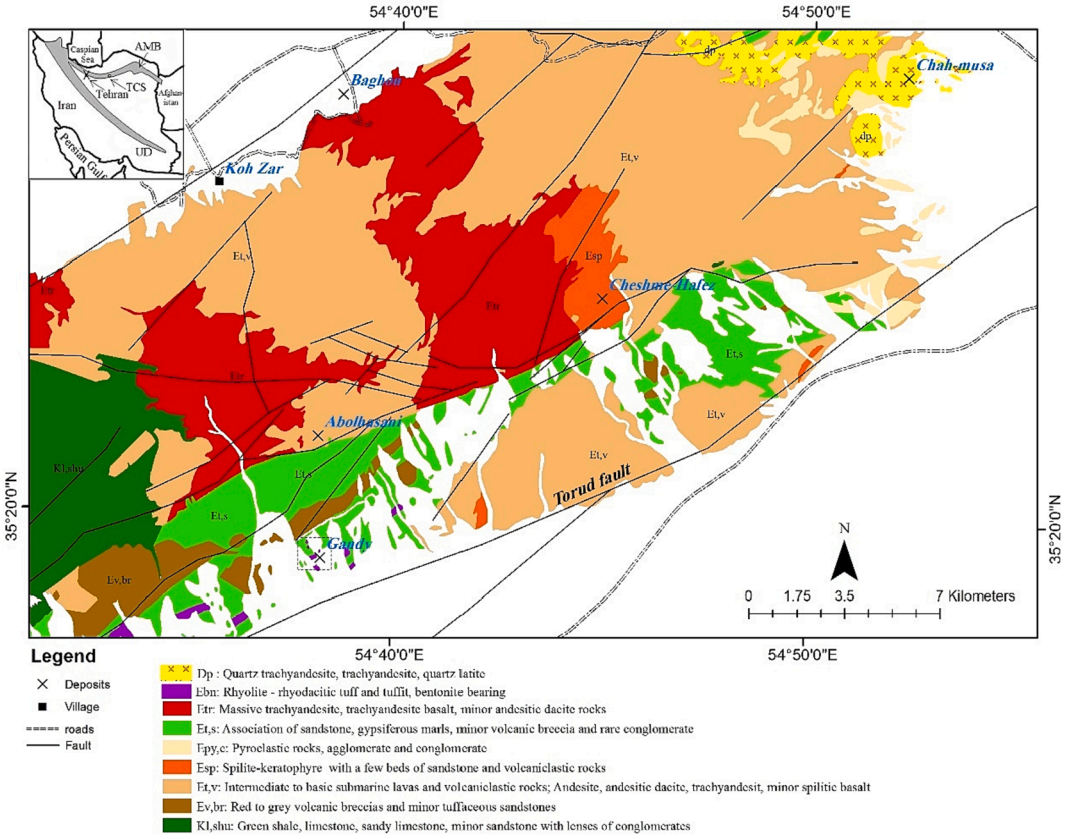

Fig. 1. Geological map of the TCS range, indicating the rock units, main areas of mineralization, and related structures (based on 1:250,000 geologic map of Toroud) (modified after Ziaii et al., 2010; Geological Survey of Iran (GSI), 1978). AMB: Alborz magmatic belt, UD: Urumieh-Dokhtar zone, TCS: Toroud-Chah Shirin range.

(Baumann et al., 2016). Big data applications use BDA techniques to efficiently analyze large amounts of data (Mohamed et al., 2020). BD has instigated research on data mining in multiple fields (e.g., Abedini et al., 2018; Chen and Wang, 2018; Tewari and Dwivedi, 2019; Sun and Scanlon, 2019).

Earth sciences are likely to benefit from BDA techniques supporting the processing of the large number of datasets (Baumann et al., 2016). Earth scientists are dedicated to extract potential information from BD to find solutions to problems of the geosciences (Zuo and Xiong, 2020). Data prediction aims to provide the prediction of geological events which is the core application of BD to extract geoscience features and integrate the geoscience variables to support decision-making (e.g., Ma et al., 2015; Baumann et al., 2016; Liu et al., 2018; Zuo et al., 2019; Zue and Xiong, 2020; Xu and Zhang, 2023). BDA brings a novel way for identifying geochemical anomalies in mineral exploration because it involves processing of the whole geochemical dataset to reveal statistical correlations between geochemical patterns and known mineralization (Zue and Xiong, 2018). Traditional methods of processing geochemical data mainly involve the identification of positive geochemical anomalies related to mineralization but ignore negative geochemical anomalies. Therefore, the identified geochemical anomalies do not completely reflect the desired geochemical signature of mineralization, leading to uncertainty in geochemical exploration (Zue and Xiong, 2018).

The growth of Big Data and Analytics techniques has promoted innovation and novel approaches to integrate mineral exploration and evaluation, leading to the development of various mining geochemistry methods for mineral exploration (e.g., Veselovskii and Meshcheryakova, 2007; Ziaii et al., 2009a,b; Ziaii et al., 2012; Xiong et al., 2018; Zuo and Xiong, 2018; 2020; Li et al., 2020; Chen et al., 2022; Li et al., 2022; Zhang et al., 2023). There are many challenges in the task of mineral exploration and assessment of deposits using BD. The data are inherently complex and of great significance to the spatial relevance of deposits (Li et al., 2020). However, the data pattern becomes gradually complex, and the relationship among the data gradually expands along with the growth of data volume, contributing to a greater challenge to classification and prediction, and resulting in poor performance of traditional processing methods. BDA can bring new ideas for geological studies and numerous promising progresses in the exploration and assessment of mineral resources with the help of BD have been achieved. (e.g., Zuo and Xiong, 2018; Li et al., 2020):

Zhao, (2015) proposed and introduced BD concepts into geosciences, anticipated the idea that digital mineral exploration can realize a leap from mathematical geology to digital geology and fill the gaps of traditional qualitative exploration, and carried out scientific quantitative assessment and analysis on mineral prediction. Xiao et al. (2015) investigated the basic theoretical principles for the prediction and evaluation of mineral resources and summarized the major processes in the digital and information age with the help of prediction methods during the age of BD. Yu et al. (2015) proposed new geological big data-based models to quantitatively predict and evaluate mineral resources. Zheng et al. (2015) suggested that the national geological information service system could boost the share of geological information under the big data setting and balance the data service and information knowledge service. Chong and Shi, (2015) provided an overview of content, scope, and findings of BDA, and discussed its future evolution. Xiong et al. (2018) applied BD and a deep learning algorithm to process geoscience data to identify and integrate anomalies related to skarn-type iron mineralization. The results demonstrated that BD supported by deep learning methods is a potential technique to be considered for use in MPM. Zuo and Xiong (2018) identified the geochemical anomalies related to Fe polymetallic mineralization through BD of regional geochemical stream sediment, with the support of machine learning methods. Zuo and Xiong (2020) conducted a case study on geochemical

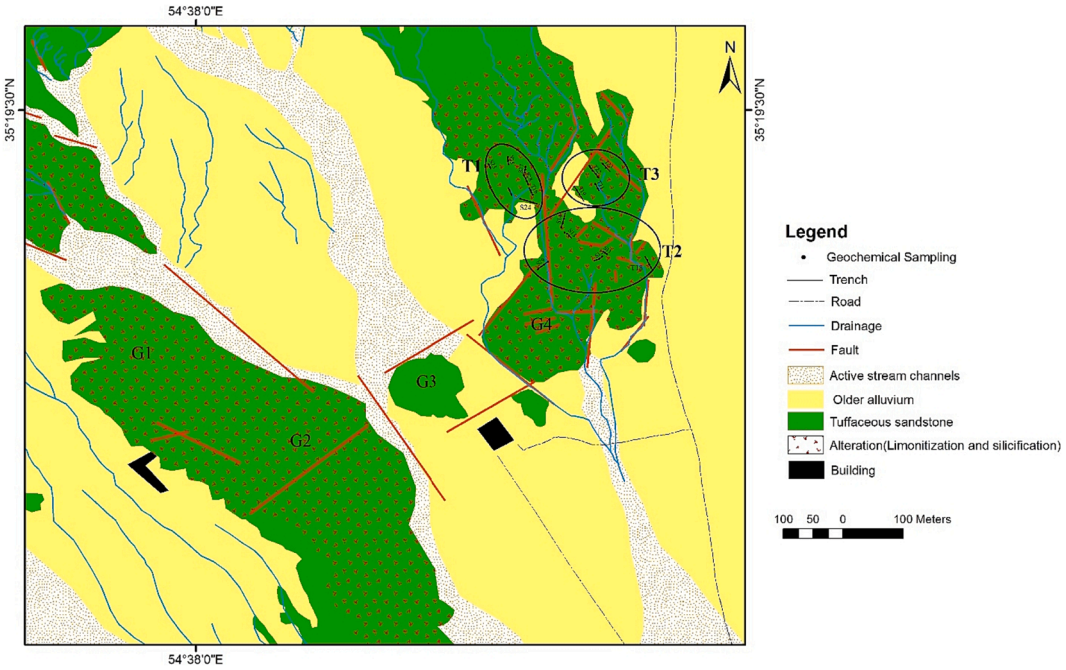

Fig. 2. Geological map of the Gandy deposit.

exploration data mapping, using Geoscience BD and concluded that geoscience BD is a new research paradigm to investigate the spatial association of geochemical patterns, mining elemental association, and recognizing geochemical anomalies associated with mineralization via geo-computation and geo-visualization techniques in support of mineral exploration. Li et al. (2020) used geological BD and deep convolutional neural network to extract spatial distribution characteristics and the relevance of various ore-controlling factor layers. Chen et al. (2022) used BDA based on big geochemical data (5683 samples) and machine learning technique to predict the tectonic background more accurately. Li et al. (2022) investigated the development of intelligent methods for mineral resource prediction under the background of geological BD. Zhang et al. (2023) demonstrated a general method based on remote sensing data (e.g., big data) and machine learning technique to provide a form of secondary geochemical data that integrates the most desirable aspects of remote sensing data.

Gold potential metallogenic belts around the world have been identified by Safonov (1997), and two main gold metallogenic belts have been located in Iran: the NW-trending Urumieh-Dokhtar zone, and the Alborz magmatic belt in northern Iran. These belts continue to neighbor the Zod gold mine, the largest in Armenia and Azerbaijan (Safonov, 1997). The NE-trending TCS belt is located in the central to the eastern part of the Alborz magmatic belt (Fig. 1), which has a complex tectonic, magmatic, and stratigraphic history (Alavi, 1996; Shamanian et al. 2004; TaleFazel et al. 2019). The Gandy deposit is located in the southern part of the TCS (Figs. 1 and 2). It is in the Moaleman area and positioned at ~ 300 km east of Tehran. The exposed veins of this deposit have been exploited. Because of exploration issues, this mine was abandoned During 2004–2020. Various problems have to be overcome for exploration of such buried deposits in covered regions, such as indirect and weak geo-information related to buried deposits acquired from geochemical surveys due to complex overprinting relationships arising from multi-formational mineralogical and geochemical processes; and incomplete and poor coverage of geo-information due to masking effects and monomineral sampling difficulties (Cheng, 2012). The regional geochemical survey covered 42000 km^2 in north-central Iran was carried out during 1993–1995 by the Ministry of Mines and Metals of Iran and Jiangxi company, China, producing 26 map sheets at a scale of 1:10000, including the TCS range. The results of the evaluation of precious metal anomalies indicated Au, Cu, Pb, and Zn as the main prospecting elements, also five prospective districts including Gandy for detailed prospecting (Ministry of Mines and Metals of Iran, 1996). Subsequent works have identified these districts as epithermal-type prospects. To date, some studies have been conducted on the Gandy deposit (Badakhshanmomtaz, 2003; Ziaii et al., 2010) and nature and genesis of Gandy were not studied in detail (TaleFazel et al., 2019). Shamanian et al. (2004) indicated that Gandy is divided into (I) brecciation, (II) fracture filling, and (III) crustiform banding. In stage I, native gold is commonly found within partially oxidized pyrite and secondary iron oxides and hydroxides and coexists with galena and chalcopyrite in stage II. Fard et al. (2006) indicated that alteration and mineralization have occurred in two stages that resulted in the formation of the argillic alteration and brecciation of the host rock; and precious and base metal mineralization, respectively. Keynejad et al. (2011) and Rezaeeshahzadeh et al. (2012) introduced three principal fault and fracture systems including NE-SW, NW-SE, and E-W trending. They concluded that mineralization has occurred along faults and fractures and most mineralized veins are controlled by NE-SW and E-W trending fractures.

In this research, BDA based on mineralogical and geochemical type (MGT) modeling were applied to process geoscience big data and identify geochemical anomalies associated with multi-MGT gold mineralization in the Gandy deposit. The buried, hidden and deep ore bodies were explored using mining geochemistry approaches presented in this study. Also, the exploration challenges of the Gandy deposit were solved using the BDA developed in this research.

2. Geological setting of study area

2.1. Regional geology

There are two main gold metallogenic belts have been located in Iran (Safonov, 1997): the NW-trending Urumieh-Dokhtar zone, which runs parallel to the Zagros thrust, and the Alborz magmatic belt in northern Iran. The NE-trending Toroud-Chah Shirin (TCS) belt, which lies in the central to eastern part of the Alborz magmatic belt (Alavi, 1996; Shamanian et al. 2004; TaleFazel et al. 2019), is the largest known gold and base metal province of Iran (Safonov, 1997). Alavi (1991 and 1996)

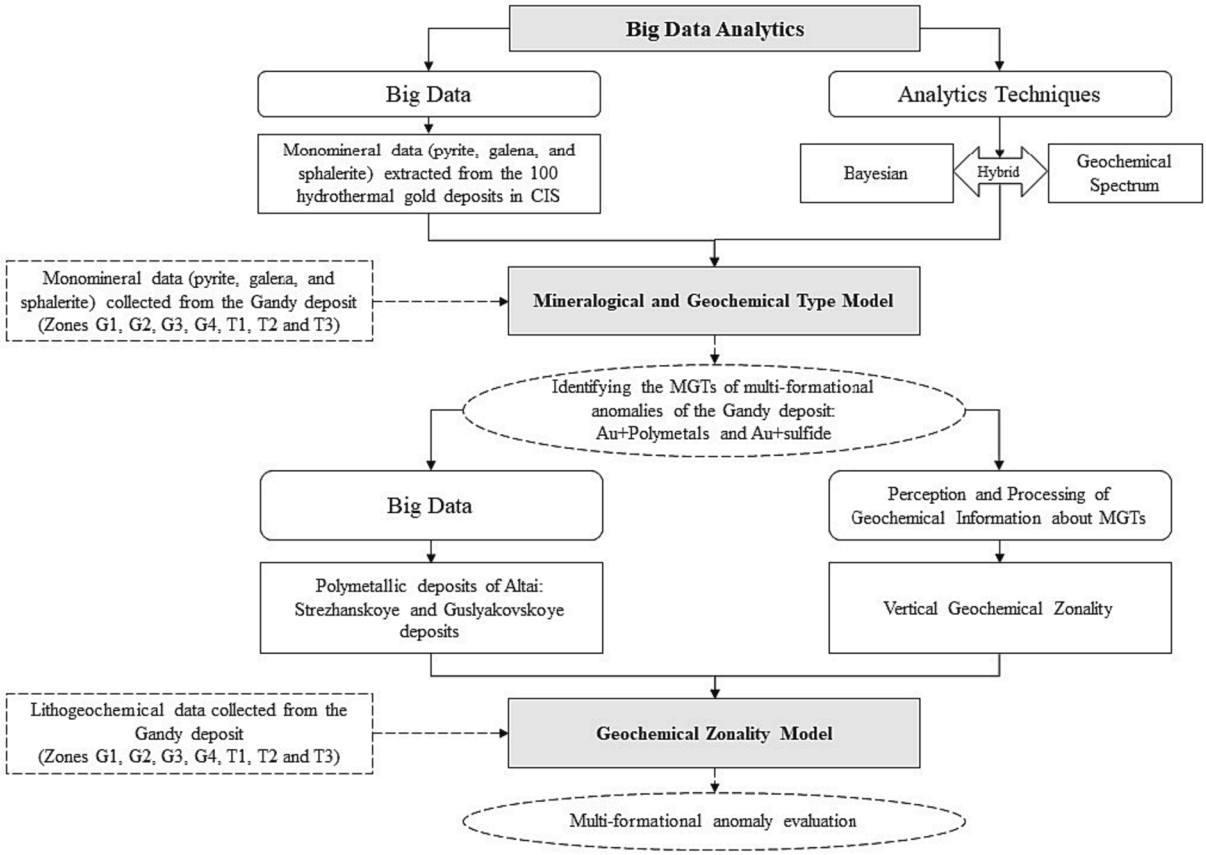

Fig. 3. Graphical representation of workflow used in this research.

suggested that the TCS range is related to the Eocene magmatism in the Central Iran magmatic zone to the south (Alavi, 1991; Alavi, 1996; Shamanian et al. 2004; TaleFazel et al. 2019). The Tertiary igneous rocks show that the western part of the Alborz belt merges with the Urumieh-Dokhtar zone (Shamanian et al. 2004). Hassanzadeh et al. (2002) suggested that the two belts were once a single arc but separated by intra-arc extension that started in the late Eocene (Hassanzadeh et al. 2002; Shamanian et al. 2004). According to the recent review, the Alborz belt includes TCS. TCS range mainly consists of Eocene volcanic and pyroclastic rocks and equivalent subvolcanic and intrusive bodies, although there are scattered outcrops of metamorphosed Paleozoic and Mesozoic rocks. Structural patterns are controlled by two principal strike-slip faults, Anjilow in the north and Toroud in the south, both with NE trending as shown in Fig. 1.

TaleFazel et al. (2019) suggested that orthogonal subduction of the Lut microplate beneath the Turan Plate may have played a significant role in sulfide mineralization. The strike-slip faults movement may also have been important in the ore-forming process. The ore-forming fluids were mainly of magmatic-hydrothermal origin (e.g., Gandy). According to the distribution of mineralized systems in the TCS arc, the majority of the ore deposits are epithermal (e.g., Tale Fazel et al., 2019; Eskandari et al., 2023). The presence of geochemical anomalies and ore deposits showing abandoned mines with similar epithermal characteristics suggests that the TCS range is prospective for high-grade gold veins and base metal epithermal deposits (Shamanian et al., 2004).

2.2. Local geology

The Gandy epithermal deposit is located in the TCS belt (Fig. 1). The local stratigraphy from oldest to youngest includes the following: (1) A sequence of thin-bedded volcaniclastic siltstones and sandstones in the lower section, Rhyolitic tuffs and tuffaceous sandstones in the upper part (Hushmandzadeh et al., 1978; Shamanian et al., 2004); (2) Lapilli tuffs, volcanic breccias, and intermediate lava flow unconformably overlie the lower unit; (3) Rhyolitic to rhyodacitic domes of Eocene or much younger (Shamanian et al., 2004). The fractures and faults have N 50° to 60° E strikes and 50° to 80° SE dips and were formed by movement on the NE-trending Toroud fault (Shamanian et al., 2004).

2.3. Mineralization

Mineralization of the Gandy Au–Ag ± Pb–Zn deposit occurs as shallow, massive lens-shaped bodies and as steeply dipping veins and breccias. The veins and breccias consist of galena, sphalerite, pyrite, chalcopyrite, quartz, barite, and carbonate minerals and is accompanied by alteration halos of quartz, illite, and calcite. The breccias include economically important gold and base metal sulfides. The veins include quartz-carbonate assemblages and economically important but narrow veins of base metal sulfides. The main ore minerals are chalcopyrite, pyrite, sphalerite, galena, and chalcocite. The gangue minerals are quartz, barite, calcite, dolomite, chlorite, sericite, chalcedony, and epidote. In the vicinity of the mineralization, the host rocks are altered to kaolinite–sericite–carbonate ± chlorite (Shamanian et al., 2004; Fard et al., 2006; TaleFazel et al., 2019). Native gold occurs within partially oxidized pyrite and secondary iron oxides such as goethite, in breccias. Also, gold grains coexist with galena, chalcopyrite, and their supergene alteration products, such as cerussite and chalcocite, in the fracture-filling structures (Shamanian et al., 2004). The chemical composition of samples taken from veins of the Gandy deposit was investigated and the result showed positive correlations between Zn and Au.

3. Materials and methods

Fig. 3 demonstrates the methodological flowchart to identify and

assess the multi-MGT geochemical anomalies in the Gandy gold deposit.

3.1. Big data analytics (BDA)

BD is defined as a new generation of technologies and architectures, designed to economically extract value from huge volumes of a wide variety of data, by enabling high-velocity data capture, storage, discovery, and/or analysis' (Gantz and Reinsel, 2012; Zakir et al., 2015). Some researchers define big data based on its attributes:

The concept of BD given by Doug Laney (2001) was characterized by volume (consisting of enormous quantities of data), velocity (created in real-time), and variety (being structured, semi-structured and unstructured), acknowledged as 3Vs (Zakir et al., 2015; Tsai et al., 2015; Kitchin and McArdle, 2016). It points out that big data does not simply mean large datasets (big Volume) but also efficient dataset management (big Velocity) and great heterogeneity (big Variety) (Baumann et al., 2016). However, the concept of D. Laney was expanded to five characteristics (5Vs), namely, volume, velocity, variety, value, and veracity (Qiu et al., 2016; Nti et al., 2022). The first "V" (volume) denotes the data size. The second "V" (velocity) refers to the changing rate of the data. The third "V" (variety) denotes the multiplicity, heterogeneity, and diverse formats of data and different kinds of uses and ways of analyzing the data. The fourth "V" (value) is the most essential and irreplaceable characteristic because of the power to transmute data into a piece of valuable information. The fifth "V" (veracity i.e. addressing quality and uncertainty) (Baumann et al., 2016) refers to the credibility of the data (Nti et al., 2022). These definitions highlight the challenges researchers face when processing big data.

The reason is that earth sciences raise significant challenges in terms of storage and computing capabilities, as: (1) Earth sciences include a wide range of applications: (e.g., Geology) and make use of heterogeneous information (Big Variety): covering a diverse temporal range (e.g., geological studies), supporting a wide spatial coverage, modeling many different geospatial data types; (2) Earth sciences are based on observations and measurements coming from in situ and remote sensing data (Big Volumes); (3) They make use of complex scientific modeling to study complex scenarios requiring fast processing (Big Velocity) (Baumann et al., 2016).

BDA practically involves big data and analytics, and how these two have teamed up to create one of the current trends in mining geochemistry. BDA is applying analytical methods and techniques on big datasets to uncover patterns in geoscience BD (Baumann et al., 2016). BD are high-dimensional, diverse, gigantic, complex, incomplete, and noisy, making data pre-processing difficult in BDA. Therefore, BDA designers need to manage the data pre-processing stage (e.g., data clean, sampling, and compression) highly and efficiently (Nti et al., 2022).

The importance of applying BDA to mining geochemistry is to generate the geochemical models using different kinds of BD, to identify the characteristics of the distribution of trace element contents in monominerals, and to assess the multi-formational geochemical anomalies. BDA using full samples, instead of partial samples, permits more detailed exploratory analysis among all the available data. Mathematical methods for evaluating multi-MGT geochemical anomalies commonly focus on separating anomalies from the background. BDA can overcome these limitations by using the entire geochemical dataset of monomineral samples to identify multi-MGT anomalies and quantify their relations with known mineralization patterns.

The BD used to identify the MGTs of multi-formational geochemical anomalies comprises the results of the analysis of 9440 monomineral samples (i.e., 8640 samples of pyrite, 362 samples of galena, and 438 samples of sphalerite) extracted from the 100 hydrothermal gold deposits in CIS (collected by S.V. Grigorian, T.T. Liakhovich, M. Ziaii, and I.I. Getmansky) (Ziaii, 1999; Grigorian et al., 1999a, 1999b; Grigorian and Liakhovich, 2000).

According to the obtained MGTs from MGT models, the databank used to assess the multi-formational anomalies comprises the polymetallic deposits of Altai (i.e., Guslyakovskoye deposit) (collected by M. Ziaii under the supervision of S.V. Grigorian) (Ziaii, 1999). These geochemical BD has been used to assess the multi-MGT geochemical anomalies related to gold mineralization.

3.2. Methodology

The essential factors for the identification of geochemical anomalies can be categorized into the geochemical landscape, mineralogical and geochemical type (MGT) of anomalies, and geochemical zonality (Sochevanov, 1961; Ziaii et al., 2011; Ziaii et al., 2012; Zuo et al., 2016; Macheyeki et al., 2020; Heidari et al., 2021). Recognition of hydrothermal alteration zones has no critical role to distinguish blind mineralization (BM) from zone dispersed mineralization (ZDM) at a local scale (Ziaii et al., 2009a; Timkin et al., 2022). The multi-MGT anomalies associated with gold mineralization were formed by complex geochemical processes, with many geochemical elements from the host and source rocks involved in water–rock interactions, leading to complex geochemical patterns.

3.2.1. Geochemical landscape

The concept of geochemical landscape, defined by Perelman (1975), refers to an epigenetic zone where the conditions of elemental migration were markedly changed, leading to a significant accumulation of certain elements. The geochemical landscape is identified according to the physical and chemical properties of soil, vegetation characteristics, natural moisture conditions, groundwater level, the mineralogical composition of soil and underlying rocks, and the presence or absence of anthropogenic impact.

The geochemical landscape conditions of the TCS belt (e.g., Gandy area) are mountainous and arid landscapes. The main characteristics of arid landscape posing problems to geochemical exploration are as follows: eliminating the geochemical response by considerable admixtures of aeolian materials; producing false anomalies by mechanical barriers where minerals with higher specific gravity, unrelated to true anomalies may be concentrated; the predominance of mechanical weathering over chemical weathering; poorly developed drainage systems; changes of optimum grain fraction size from rugged regions to peneplain areas. The results of studies conducted by many researchers have shown that statistical methods are not satisfactory to recognize geochemical anomalies due to the complex geochemical conditions in arid landscapes (e.g., Arkhipov et al., 1990; Ziaii et al., 2007; Kuzmenkova, and Vorobyova, 2015).

There are two coefficients to describe the features of a geochemical landscape: the mineralization coefficient (Cm) and the productivity coefficient (K). If it is assumed that among samples collected along a profile $(\eta_A(\alpha))$, $\eta_A(\alpha)ore$ is the number of samples identified as abnormal and falling inside the contour of a mineralization zone. The mineralization coefficient (Cm) can defined as follows (Grigorian, 1985):

$$\mathrm{Cm} = \frac{(\eta_{\mathrm{A}}(\alpha)\mathrm{ore})}{(\eta_{\mathrm{A}}(\alpha))} \tag{1}$$

Both coefficients are used to calculate the vertical geochemical zonality coefficient (Vz) (Grigorian, 1985; Solovov, 1987; Arkhipov et al., 1990).

$$\mathrm{Vz} = \frac{\mathrm{Cm_{Ba}} \times \mathrm{Ba} \times \mathrm{Cm_{Ba}} \times \mathrm{Ba}}{\mathrm{Cm_{Ni}} \times \mathrm{Mo} \times \mathrm{Cm_{Ni}} \times \mathrm{Ni}} \tag{2}$$

In this research, considering the mentioned features, the mineralization coefficient (Cm) was used to create the geochemical zonality (Vz) models for evaluating the multi-formational geochemical anomalies in the Gandy area. This approach has allowed the conditions of migration and accumulation of Cm in the Gandy deposit to be revealed and assisted in the understanding of migration and accumulation conditions of Cm.

The mining geochemistry geo-information system has been developed for studying the distribution features of technical sampling in arid

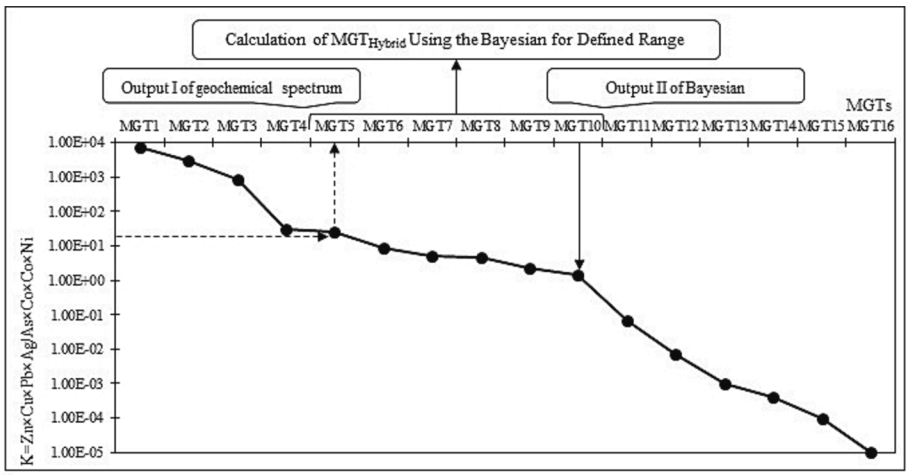

Fig. 4. Graphical representation of the hybrid model construction for a hypothetical monomineral.

terrains. A series of landscape-geochemical maps was made at local and regional scales, and the Cm conditions were determined in the study area. The data processing and map production used a variety of geo-information technology (Auto CAD 3D map, ArcGIS). This approach allowed (1) a spatial analysis of technical sampling distribution in the arid relief; (2) the extracted information to be summarized, and (3) different mapping layers and attribute data to be combined. For this purpose, a special object-oriented mapping database of relief data, environmental and mining geochemistry properties, and specification of technical migration and accumulation of the study area, were developed.

3.2.2. Mineralogical and geochemical type (MGT) of anomalies

The quantitative evaluation of multi-formational anomalies is applied using the mineralogy and chemistry of ores and primary haloes in the deposits and geochemical anomalies (Ziaii et al. 2012). In this study, three analytical techniques were utilized to identify the relation between the trace element contents of monominerals (e.g., BD) and MGTs of anomaly. There are three components to apply these methods: (1) a database of trace element contents in monominerals of gold deposits or MGT, (2) a database on a geochemical anomaly area, and (3) a data analytical technique (Ziaii et al., 2009b). The trace element contents of monomineral of the gold deposits allowed discrimination between the various MGTs.

The classification of gold deposits is an intricate problem because of the complexity of the gold element. The trace elements (e.g., Au) may be concentrated as the primary or secondary haloes in endogenic and exogenic deposits with multi-formational types. Although the big data of trace elements contents in monominerals are available in world literature, their dispersion and concentration patterns have not been investigated.

3.2.2.1. Bayesian method. The study of Bayesian method is aimed at mastering the Bayesian approach to probability theory as one of the consistent methods of mathematical reasoning under uncertainty. In the Bayesian approach, probability is interpreted as a measure of ignorance rather than objective randomness. Simple rules, such as the total probability formula and Bayes' formula, allow reasoning under conditions of uncertainty. On this basis, the Bayesian approach to probability theory can be considered as a generalization of classical Boolean logic. The goal is to apply the Bayesian approach to solving BD problems. The Bayesian approach makes it possible to effectively take into account various preferences when constructing decision prediction rules.

The different patterns of impurity elements in pyrite, galena, and sphalerite are coincident with the classification of gold deposit types and perhaps a result of different mineralizing processes. In this research, the Bayesian method is utilized to identify the MGT, calculate the conditional posterior probabilities, and make decision-based on a comparison of obtained magnitudes. If the number of MGT in set A is equal to m, then each object is characterized by indications. Suppose:

$$x_1 = x_1^0, x_2 = x_2^0, \ldots, x_n = x_n^0, K_n = \{x_1^0, x_2^0, x_3^0, \ldots, x_n^0\} \quad (3)$$

The probability of realization of an event Kn will be determined using Bayes' formula:

$$P(B_i|K_n) = \frac{P(B_i).f_i(x_1^0, x_2^0, x_3^0, \ldots, x_n^0)}{\sum_{i=1}^{m} P(B_i).f_i(x_1^0, x_2^0, x_3^0, \ldots, x_n^0)} \quad (4)$$

where i is class of MGT. The value of $P(B_i).f_i(x_1^0, x_2^0, x_3^0, \ldots, x_n^0)$ is dependent with the probability compound:

$$P(B_i).f_i(x_1^0, x_2^0, x_3^0, \ldots, x_n^0) = \prod_{i=1}^{n} P(B_i)f_i(x_i) \quad (5)$$

The applied method is based on the prior probability of the Bayesian. The trained classifier applies Bayes' rule to calculate the posterior probabilities of all states of the class variable and predicts the class label that takes the highest posterior probability.

3.2.2.2. Geochemical spectrum method. The method of the geochemical spectrum of elements was proposed to identify and calculate the discriminant function. This method has been used to compare two similar geochemical fields with different economic natures using simple graphical charts (Solovov and Garanin, 1968; 1972), separate different rocks in terms of geochemistry and similar formations in terms of having or not having potential (Beus and Grigorian, 1977). The results showed that the discriminant function should be simple to represent geological models. Accordingly, the following function is obtained utilizing one of the simplest discriminant functions with variables C_1 and C_2 of two similar formations or fields (I, II) (Beus and Grigorian, 1977).

$$v = \frac{(C_1)_I}{(C_1)_{II}} \quad (6)$$

This linear function can be represented by a 2D plot between C1 and C2 variables. If the ratio $(C_1)_I/(C_1)_{II} < 1$ is satisfied, this function can belong to class II for any unknown sample, and in case $(C_1)_I/(C_1)_{II} > 1$, It belongs to class I. Thus, these two classes are separated using a simple linear discriminant function in a 2D chart. The extension of this graphical method in two similar classes (each with several variables) is known as the geochemical spectrum method. The function v is a parameter which is separately calculated for each class, and if the ratio $v_1/v_2 > 1$ is satisfied, this determines the difference in the chemical combination between these two similar classes (Beus and Grigorian,

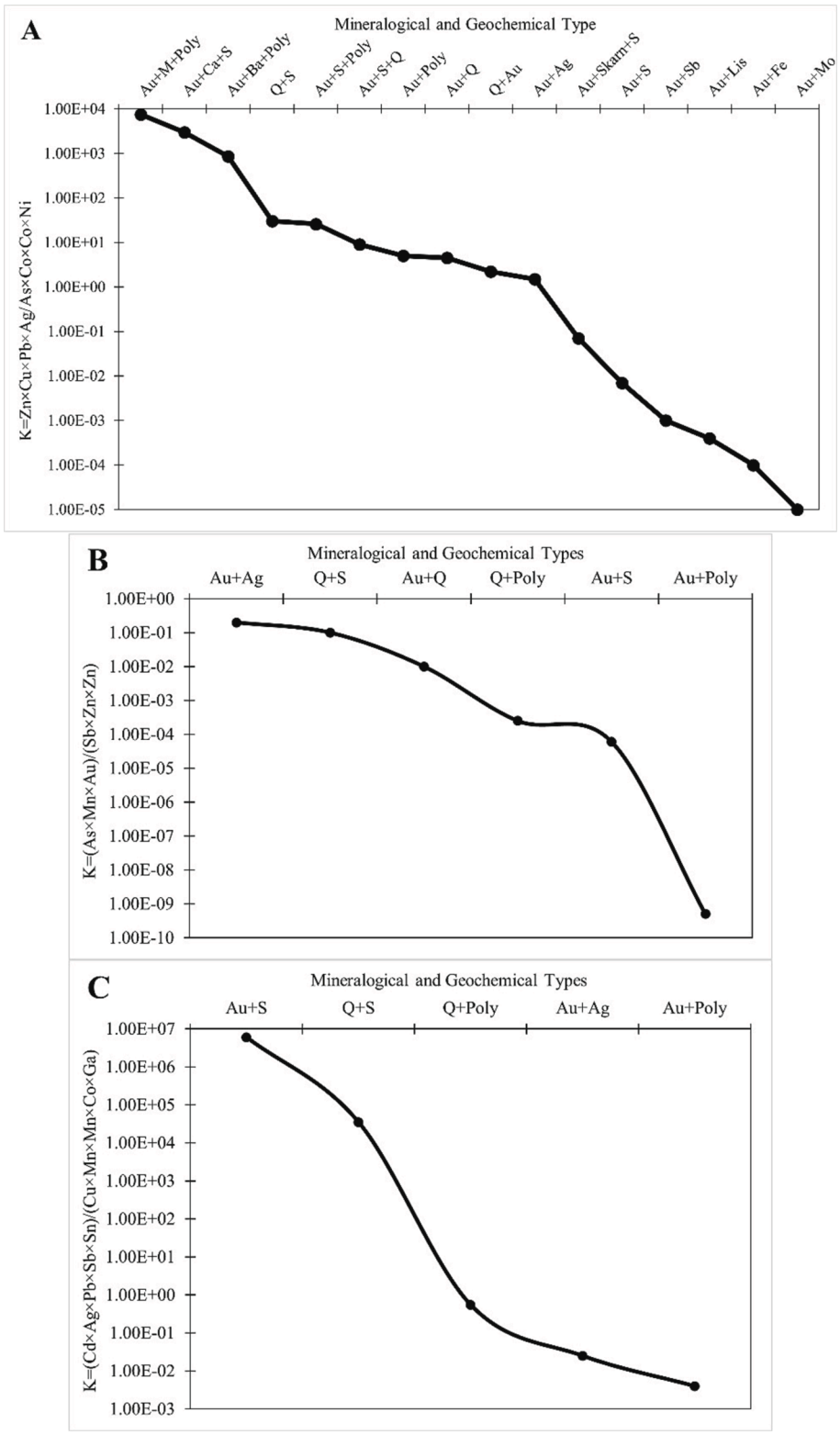

Fig. 5. The geochemical spectrum-in-MGT models for (A) pyrite - $K_{pyrite} = Zn \times Cu \times Pb \times Ag/As \times Co \times Co \times Ni$, (B) galena – $K_{galena} = As \times Mn \times Au/Sb \times Zn \times Zn$, (C) sphalerite – $K_{sphalerite} = Cd \times Ag \times Pb \times Sb \times Sn/Cu \times Mn \times Mn \times Co \times Ga$.

1977). The geochemical spectra method for monominerals is more simplified (compared to Bayesian) to determine the MGTs of gold ore occurrences.

3.2.2.3. Hybrid method. The hybrid method is constructed to improve the efficiency of the analytical techniques. The capabilities of two techniques including the Bayesian and geochemical spectrum are merged as a hybrid. The hybrid model combines the outputs of the individual techniques and thus obtains the advantages of all used techniques. The hybrid model construction is represented in Fig. 4. A group of MGT multiplicative coefficients is defined to identify a specific MGT. The determined MGTs of the Bayesian and geochemical spectrum

Table 1
Results of MGT identification for pyrite, galena and sphalerite samples collected from different zones of the Gandy deposit.

Zones	Monominerals	Probability of identification (%) using Bayesian modeling	Discriminant function using geochemical spectrum modeling	Probability of identification (%) using hybrid modeling
G1	Galena	Au + P (99.20)	1.2E-09 (Au + P, Au + S)	Au + P (74.80), Au + S (24.60)
	Sphalerite	Au + P (91.20)	2.5E + 02 (Q + S, Q + P)	Au + P (96.20), Q + S (3.80)
G2	Pyrite	Au + P (61.70)	2.5E + 02 (Au + S + P)	Au + P (67.0)
	Galena	Au + P (89.30)	2.2E-08 (Au + P, Au + S)	Au + P (98.7)
G3	Galena	Au + P (98.00)	2.1E-07 (Au + P, Au + S)	Au + P (71.60), Au + S (28.40)
G4	Galena	Au + P (88.60)	1.0E-07 (Au + P, Au + S)	Au + P (72.9), Au + S (27.1)
T1	Pyrite	Au + P (90.40)	6.66E + 00 (Au + S + P, Au + S + Q)	Au + P (99.77)
T2	Galena	Au + P (88.82)	4.62E-05 (Au + S, Au + P)	Au + P (90.25), Au + S (9.74)
T3	Pyrite	Au + S (65.14)	3.01E + 00 (Au + S + Q, Au + P)	Au + S (72.15), Au + S + Q (27.12)

models for each monomineral (e.g., pyrite, galena and sphalerite) are considered as boundaries of this group. Then, the Bayesian is applied to this group, and MGT of the hybrid model is obtained.

3.2.2.4. Vertical geochemical zonality. The vertical geochemical zonality (Vz) was revealed in the distribution of trace elements in monominerals (pyrite, galena, and sphalerite), which is recommended to evaluate the erosional level of multi-MGT geochemical anomalies of gold deposits. The Vz in the distribution of monominerals basically repeats the Vz of primary haloes. This zonality has greater contrast compared to the zonality of primary haloes. A monotonous decrease with depth was found in the values of Vz, which reflects the identical nature of both types of Vz. Due to a kind of "impoverishment" of elements of bulk samples in mineral aggregates formed in ore-bearing rocks during the mineralization, significant contents are recorded in minerals for several elements that are not detected by the same analysis in bulk samples. The alternative or combined use of high-contrast zonality in the distribution of trace elements in monominerals will improve the reliability of the assessment of ore occurrences (Ziaii, 1999).

3.3. Sampling, sample preparation and sample analysis

In this research, the rational mineralogical and geochemical sampling technique was used to evaluate the multi-MGT anomalies. Rational sampling refers to collecting, organizing, analyzing, and interpreting data in a way that makes sense in the context of data. The lithogeochemical samples were collected using a chip channel sampling method and taken from the geochemical haloes of zones (G1, G2, G3, G4, T1, T2, T3) of the Gandy deposit (Fig. 2). Using a binocular microscope, the size fraction was selected in which pyrite, galena and sphalerite were concentrated and monomineral samples were acquired. Other samples, in which the size-fraction is small, were crushed, homogenized, and divided into two parts: Ore minerals were analyzed as bulk samples. Ore mineral concentrates were examined and refined by handpicking under a binocular microscope to obtain 10 gr of high purity concentrate. Finally, the concentrates were powdered in an agate mortar (Ziaii, 1999). This ore mineral concentrates were also considered as monomineral samples. In total, 59 monomineral samples and 163 bulk samples were collected. All samples were analyzed by ICP-MS and fire assay.

4. Results and analysis

4.1. Mineralogical and geochemical type models

Big Data (Monomineral data extracted from the 100 hydrothermal gold deposits in CIS) and analytical techniques (Bayesian, Geochemical spectrum, and Hybrid) were used for the mineralogical and geochemical type modeling. The composition of impurity elements in minerals is not the same because of the differences in the methods of analysis of monomineral samples. So, only recorded elements in all MGT were considered to calculate for each monomineral. These elements are extracted from the available BD to select the most frequent elements in the monominerals. For pyrite it is: As, Co, Zn, Ni, Pb, Cu, Ag, Galena: As, Sb, Au, Mn, Zn and Sphalerite: Cd, Ag, Sb, Co, Mn, Cu, Pb, Sn, Ga. The MGT identification of gold deposits consists of the use of Bayesian, multiplicative coefficients selected by the geochemical spectra, and hybrid methods.

The Bayesian method was applied to the extracted BD on the composition of impurity elements in the most common monominerals (e.g., pyrite, galena, and sphalerite) such as posterior probabilities and

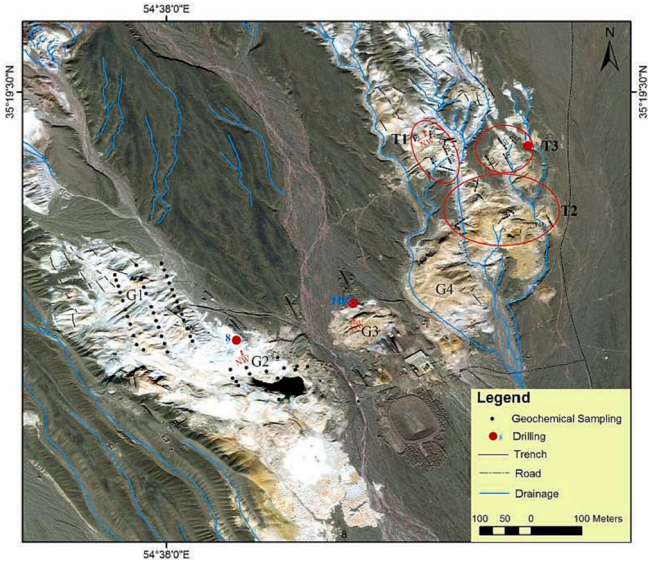

Fig. 6. The landscape-geochemical map of zones G1, G2, G3, G4, T1, T2 and T3 in the study area.

Table 2
Cm values of trace elements used for Vz models.

Zones	Cm Values of Trace Elements								
	Ag	As	Ba	Co	Cu	Mo	Ni	Pb	Zn
G1	0.03	0.14	0.19	0.22	0.08	0.17	0.05	0.03	0.14
G2	0.11	0.13	0.17	0.15	0.17	0.11	0.13	0.11	0.13
G3	0.10	0.10	0.20	0.20	0.10	0.30	0.30	0.10	0.10
G4	0.10	0.10	0.20	0.20	0.10	0.30	0.30	0.10	0.10
T	0.02	0.19	0.21	0.10	0.15	0.07	0.05	0.10	0.17

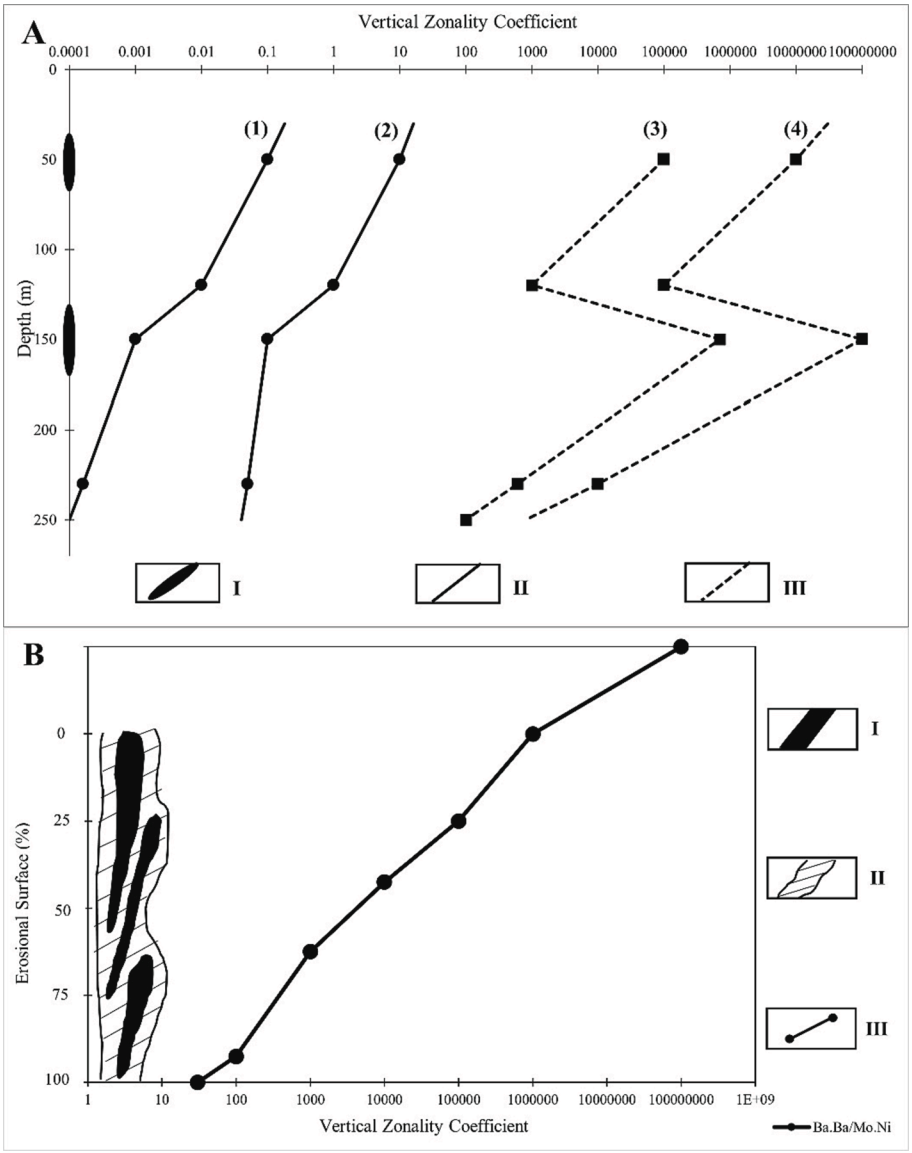

Fig. 7. The geochemical zonality models of the polymetallic deposits of Altai. (A) Strezhanskoye deposit: (1) Ba × Ag × Pb/Cu × Cu × Zn; (2) Ba × Pb/Cu × Zn; (3) Ag × Pb × Zn/Co × Ni × Mo; (4) Pb × Zn × Cu/Co × Ni × Mo; I- Ore body, II- Graphs of zonality coefficients with barium, III- Graphs of zonality coefficients without barium; (B) Guslyakovskoye deposit, I- Ore bodies, II- Ore-bearing zone, III- Graph of Ba × Ba/Mo × Ni coefficient (Grigorian, 1992).

discriminant analysis, and the relations of the trace elements in monomineral samples for each MGT were investigated. So, three MGT models based on Bayesian method have been constructed for pyrite, galena, and sphalerite. These models are referred to as the Bayesian-in-MGT models.

The geochemical spectrum method was also used to construct the MGT models. These models are referred to as the geochemical spectrum-in-MGT models. In order to process the extracted BD, the average contents of impurity elements of monominerals for each MGT were calculated. Then, graphs of discriminant functions were constructed for the distribution of average contents of impurity elements for all studied monominerals of gold deposits. According to paired comparisons of numerous graphs, the most contrasting (optimal) discriminant functions were selected to differentiate the MGT of gold deposits for pyrite, galena and sphalerite.

Fig. 5-A shows the graph reflecting the changes in the proposed discriminant function (Zn × Cu × Pb × Ag/As × Co × Co × Ni) in the 16 MGTs for pyrite. Based on the extracted analytical information on the geochemical spectrum, pyrite is geochemically the most studied for ore deposits especially for gold. So, pyrite is considered the most universal monomineral indicator for MGT identification of gold deposits. As shown in Fig. 5-A, the contrast of the change in this coefficient reaches ten orders of magnitude. The most reliably identified MGTs are the most distant from each other, using the proposed coefficient. Four MGTs including Au + polymetals, Quartz + Au, Au + Quartz, Au + Ag are the least contrasting differences from each other. Closely spaced MGTs differentiate less contrast and less reliably. So, the possibilities of other monominerals including galena and sphalerite were investigated to solve this problem.

Fig. 5-B shows the graph indicating the changes in the proposed discriminant function (As × Mn × Au/Sb × Zn × Zn) in the 6 MGTs for galena. It is quite contrasting (almost ten orders of magnitude) to differentiate the MGTs by galena. Two MGTs including Quartz + Sulfide, Quartz + Polymetals seems to be insufficiently reliable (the difference is less than one order of magnitude). So, impurity elements of reference samples for other monominerals (i.e., sphalerite) can be used to provide more reliable identification of these two MGTs.

Fig. 5-C shows the ranked graph of changes in the proposed discriminant function (Cd × Ag × Pb × Sb × Sn)/(Cu × Mn × Mn × Co × Ga) in the 5 MGTs for sphalerite. The previous mentioned MGTs differ significantly in the value of the coefficient (more than three orders of

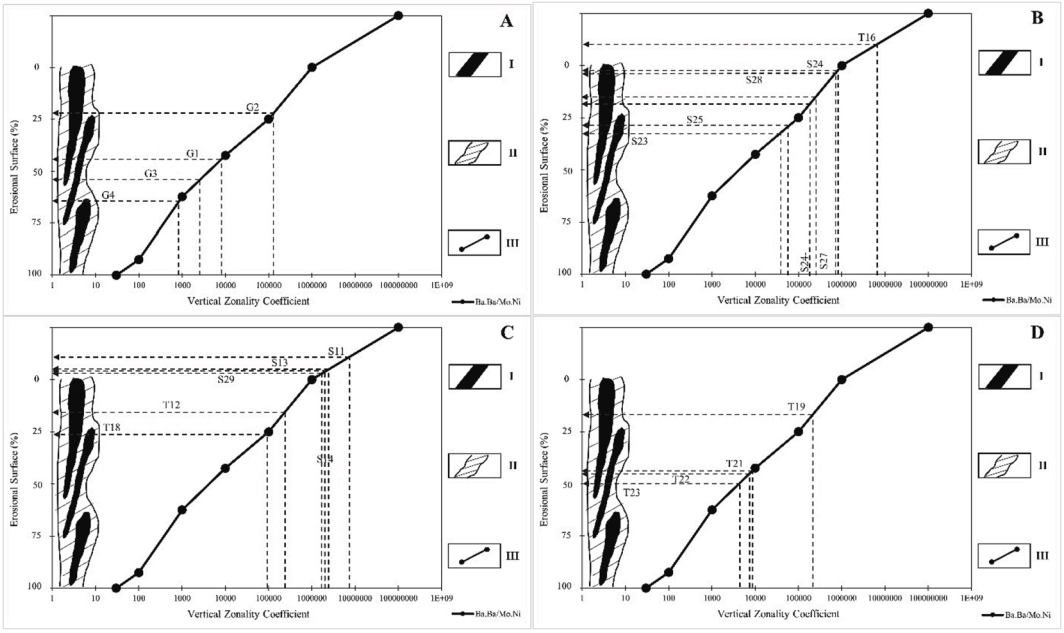

Fig. 8. Application of the standard geochemical model of the Guslyakovskoye Au + Polymetals deposit to identify the erosional surface. (A) zones G1, G2, G3 and G4, (B) zone T1, (C) zone T2, (D) zone T3.

magnitude).

The geochemical spectrum-in-MGT models for indicator monominerals can be recommended as standards for the multi-formational affiliation of geochemical anomalies. The most informative model is the standard for pyrite (16 MGTs). For other monominerals, standards have been created for a smaller number of MGT (6 and 5 MGTs for galena and sphalerite, respectively). These models can be implemented for the preliminary identification of MGT of gold deposits (Ziaii, 1999).

The MGT models based on Bayesian, geochemical spectrum, and hybrid methods for pyrite, galena and sphalerite were applied to identify the MGTs of multi-formational anomalies of the Gandy deposit (Table 1).

The Bayesian-in-MGT model was utilized to calculate the probabilities of MGT on a scale of 16 MGTs for pyrite samples collected from zones G2, T1 and T3. Based on the results, Au + Polymetals MGT was identified with the maximum value of probability. Also, the geochemical spectrum-in-MGT model was used to calculate the most effective discriminant function (Zn × Cu × Pb × Ag/As × Co × Co × Ni) for pyrite samples (see Fig. 5-A). The MGT model based on hybrid was constructed to acquire the advantages of Bayesian and geochemical spectrum methods. So, the group of MGTs was specified and the MGT probabilities of this group were determined. As shown in Table 1, the Au + Polymetals and Au + S MGTs were identified.

The Bayesian-in-MGT model was used to determine the probabilities of MGT on a scale of 6 MGTs for galena samples collected from zones G1, G2, G3, G4 and T2 of Gandy deposit. Based on the results, the probability of Au + Polymetals MGT is more than 80% in most cases. Also, the geochemical spectrum-in-MGT model was used to calculate the proposed discriminant function (As × Mn × Au/Sb × Zn × Zn) for galena samples (see Fig. 5-B). Then, the MGT model based on hybrid was utilized to identify the group of MGTs and obtain the MGT probabilities of this group. As shown in Table 1, the probability of Au + Polymetals MGT is more than 70% and the Au + Polymetals and Au + S MGTs were identified.

The Bayesian-in-MGT model was utilized to obtain the probabilities of MGT on a scale of 5 MGTs for sphalerite samples taken from zone G1 of the Gandy deposit. Based on the results, the probability of Au + Polymetals MGT is 91.20%. Also, the geochemical spectrum-in-MGT model was used to calculate the discriminant function (Cd × Ag × Pb × Sb × Sn/Cu × Mn × Mn × Co × Ga) for sphalerite sample (see Fig. 5-C). Then, the probabilities of the MGT group specified by hybrid model were determined. As shown in Table 1, Au + Polymetals MGT was identified with a probability of 96.20%. The results of analyzing 59 monomineral samples of pyrite, galena, and sphalerite from the Gandy deposit show a multi-MGT anomaly superposition that is a combination of two MGTs: Au + Polymetals and Au + sulfide.

4.2. Geochemical zonality models

In this research, the mineralization coefficients (C_m) were calculated for different zones of the Gandy deposit (Table 2). These were used to calculate the vertical zonality coefficient. Therefore, the geochemical landscape of the TCS (e.g., the Gandy area) were considered to create the geochemical zonality (Vz) models for assessing the multi-MGT anomalies.

Several ore mineralization including NE-SW, E-W and NW-SE-trending anomalies that are reflecting the underlying geological structures have been recognized (Fig. 6).

Fig. 7-A and 7-B show the standard geochemical zonality models for databank of the polymetallic deposits of Altai. Fig. 7-A shows the Vz model of the primary haloes of the Strezhanskoye deposit with depth. The graphs 3 and 4 give a sharp inflection, clearly indicating the echelon location of the ore bodies. In contrast, the graphs of the Vz with the participation of barium are strictly monotonous and do not reflect the echelon nature of mineralization. Barium shows a tendency of accumulation in the upper parts of the ore zones to form 'caps' over the ore body, in contrast to the other supra ore elements (i.e., Antimony, Silver, etc.). So, the changes of the Vz with the participation of barium (in combination with other elements) with depth is more monotonic (Grigorian, 1992).

Fig. 7-B shows the Vz model of the primary haloes of the Guslyakovskoye deposit with depth. Despite the complex echelon structure of the ore-bearing zone, this graph shows a monotonous decrease in the Vz with depth. The exceptionally high contrast of this Vz with barium was noted. The value of the Vz decreases monotonically by more than 10 million times, which ensures high reliability of using this model to evaluate the erosional surface of the whole ore-bearing zone. The described features of barium have been established at some gold

Fig. 9. Exploration of Buried and hidden mineralization in the eastern part of zone G2 in the Gandy deposit. I- Mineralization (orebody), II- Primary halo, III- Bedrock, IV- Weathering crust (Soil) and secondary residual halo, V- Alluvium, VI- The multiplicative indicator of supra-ore elements (Ba × Ba), VII-The multiplicative indicator of sub-ore elements (Mo × Ni).

deposits (Grigorian, 1992).

The standard Vz model of the Guslyakovskoye Au-Polymetals deposit in Kazakhstan (Fig. 7-B) was utilized to evaluate the multi-formational geochemical anomalies of the Gandy deposit and identify their erosional surface. Values of Vz decrease downward uniformly, suggesting the existence of uniform Vz in primary halos of Au-Polymetals deposit. Therefore, vertical variations of Vz allow the distinction of mineralization levels and their primary halos (supra ore, upper-ore, ore, lower-ore, and sub-ore). The exploration importance of the Vz is to recognize the erosional surfaces indicating vertical levels of geochemical anomalies. high values of the Vz imply the presence of subcropping deposits, whereas low values of the coefficient imply outcropping or already eroded deposits.

The quantitative uniform geochemical zonality model of the Guslyakovskoye gold Polymetals deposit was used for the interpretation of the results of geochemical sampling in the Gandy deposit. This standard model was utilized to identify the erosional surface in zones G1, G2, G3, G4, T1, T2 and T3 of the Gandy deposit. The zonality coefficients were calculated to assess the ore potential of these multi-formational geochemical anomalies and the results were plotted in Fig. 8.

Zones G1, G2, G3 and G4: The geochemical anomaly G1 is the western flank of the Gandy deposit. The plot of the Vz on the standard geochemical model (Fig. 8-A) shows zone G1 is promising to the depth. The value of the Vz is very high and blind mineralization exists in this zone. Zone G2 is the southeastern flank of zone G1. It can be seen from Fig. 8-A that the value of the Vz is the highest. It means that a supra-ore geochemical anomaly exists in this zone, so, zone G2 is considered promising for blind mineralization. Zones G3 and G4 are located next to each other in the northeastern flank of zone G2. In these zones, the values of the Vz imply outcropping mineralization (Fig. 8-A).

Zone T1, T2, T3: Zones T1 and T3 are located next to each other in the north flank of zone T2. The plots of the Vz on the standard model (Fig. 8-B and 8-C) show zones T1 and T2 are promising to the depth. According to the high values of the Vz, blind mineralization exists in zones T1 and T2. In zone T3, the values of the Vz indicate outcropping mineralization (Fig. 8-D, Fig. 6: BH 11).

5. Discussion and conclusions

Big data, which has become a new scientific paradigm in the 21st century, gives rise to geoscience big data, i.e. mathematical and quantitative geoscience. The main function of monomineral big data is to

manage various mineralogical and geochemical types of data that come from different multi-MGT geochemical haloes. With more and more data being generated, processing large amounts of data in an acceptable time has become a major challenge. In order to efficiently extract value from monomineral big data, big data analytics has become a key factor to reveal hidden information in this big data. Mining geochemistry has created and developed a variety of local and mine scale resource prediction and assessment methods, achieving beneficial practical results. Big data analytics has the potential to impact many facets of mining geochemistry. The previous (traditional) mathematical methods for identifying the multi-formational anomalies commonly focus on separating anomalies from the background. Big data analytics can overcome these limitations by using the entire geochemical databank to identify the multi-formational anomalies and quantify their correlations with known mineralization patterns.

In this research, a new approach for gold-identification of geochemical anomaly (IGA) determination was introduced. The proposed methodology, which is based on monomineral big data and Bayesian, Spectrum and Hybrid (BSH) model is quite inexpensive compared with the other exploration methods. There is more than one hundred gold-IGA in the Gandy deposits with different MGTs. The following steps were performed based on the BSH model in mining geochemistry: (1) Identification of mineralogical and geochemical types (Table 1); (2) Geometrical identification of gold-IGA (shown in Fig. 9). The dip direction of the ore body is determined by the direction of displacement of the epicenter of the multiplicative indicator of sub-ore elements from the ore-bearing structure which will correspond to the fall of mineralization; (3) evaluation of the erosional surface of the gold-IGA; (4) Priority ranking of each gold-IGA based on their gold reserves. It is worth mentioning that there is the main ore system of structure and geometrical gold-IGA which has N 50 to 60 E strike and 50° to 80° SE dip according to the results of the previous studies (e.g., Shamanian et al., 2004). These four steps were implemented in the Gandy deposit in 2021. The results led to the exploration of another ore system that has N 70 to 80 E strike and 50 NW dip in zone G2. According to the geochemical zonality model (Fig. 8-A), zone G2 is considered blind and hidden mineralization (Fig. 9). Exploratory drilling with 15° angle (Figs. 2 and 7, BH 8) in the north of zone G2 has intersected the ore body at a depth of 130 m and confirmed the results of this research. Also, two other ore bodies (i.e., zones G3: BH 2402 and zone T1) are categorized in this new ore system (Figs. 2 and 6). During the past two years, the results of exploitation up to a depth of 50 m in zones G2, G3 and T1 have confirmed the results of this research. The feasibility study, based on the proposed approach for gold-IGA, shows effective and useful results. It has been demonstrated that in gold multi-MGT mineralization, an application of a carefully designed and elaborated BSH model can provide acceptable results.

Appropriately, the proposed approach in this research has revealed multi-MGT geochemical anomalies in the Gandy deposit and the possibilities for the occurrence of blind mineralization related to these anomalies were evaluated. The results obtained from applying the new proposed methodology to the Gandy deposit reveals significant improvements, comparing the results obtained from previous studies (e.g., Shamanian et al., 2004; Fard et al., 2006; TaleFazel et al., 2019). Computationally, the introduced technique makes it possible, without exploration drilling and time-consuming procedures to distinguish between zones of dispersed ore mineralization and blind mineralization.

Declaration of Competing Interest

The authors declare that they have no known competing financial interests or personal relationships that could have appeared to influence the work reported in this paper.

Data availability

The authors do not have permission to share data.

Acknowledgments

The research was supported by the School of Mining, Petroleum and Geophysics Engineering at the Shahrood University of Technology. The authors are grateful to M. Ziaei, CEO of Faravar Kanyab Gisoum Co., for financial support and useful suggestions which helped us to introduce a new branch of mining geochemistry. The School of Earth Sciences & Engineering, Tomsk Polytechnic University is acknowledged for financial support for open-access publication. The Institute of Oceanography and Environment (INOS), Universiti Malaysia Terengganu (UMT) is also acknowledged for providing facilities for editing, rewriting, and reorganizing the manuscript.

References

Abedini, M., Ziaii, M., Negahdarzadeh, Y., Ghiasi-Freez, J., 2018. Porosity classification from thin sections using image analysis and neural networks including shallow and deep learning in Jahrum formation. J. Mining Environ. 9 (2), 513–525.

Alavi, M., 1996. Tectonostratigraphic synthesis and structural style of the Alborz mountain system in northern Iran. J. Geodyn. 21 (1), 1–33.

Alavi, M., 1991. Tectonic map of the Middle East, scale 5,000,000. Geological Survey of Iran (GSI).

Arkhipov, A.Ya., Bugrov, V.A., Vorobyov, S.A., Gershman, D.M., Grigorian, S.V., Kiyatovsky, E.M., Matveev, A.A., Milyaev, S.A., Nikolaev, V.A., Perelman, A.I., Solovov, A.P., Shvarov, Yu.V., Yufa, B.Ya., Yaroshevsky, A.A., 1990. Handbook of geochemical prospecting for minerals. Nedra, Moscow, 335p. (in Russian).

Badakhshanmomtaz, G., 2003. geological map of the Gandy Deposit. Ministry of Industries and Mines, Semnan Province.

Baumann, P., Mazzetti, P., Ungar, J., Barbera, R., Barboni, D., Beccati, A., Bigagli, L., Boldrini, E., Bruno, R., Calanducci, A., Campalani, P., 2016. Big data analytics for earth sciences: the Earth Server approach. Int. J. Digital Earth, 9(1), 3-29.

Beus, A.A., Grigorian, S.V., 1977. Geochemical Exploration Methods for Mineral Deposits. Applied Publishing, Wilmette.

Chen, L., Wang, L., 2018. Recent advance in earth observation big data for hydrology. Big Earth Data 2 (1), 86–107.

Chen, Z., Wu, Q., Han, S., Zhang, J., Yang, P., Liu, X., Lang, M., 2022. The metallogenic tectonic implication of the volcanic rocks of the Dahalajunshan Formation in the Early Carboniferous in the West Tianshan based on big data analytics. Arab. J. Geosci. 15 (22), 1658.

Cheng, Q., 2012. Singularity theory and methods for mapping geochemical anomalies caused by buried sources and for predicting undiscovered mineral deposits in covered areas. J. Geochem. Explor. 122, 55–70.

Chong, D., Shi, H., 2015. Big data analytics: a literature review. J. Manage. Anal. 2 (3), 175–201.

Eskandari, M., Sheibi, M., Mousivand, F., Lehmann, B., 2023. Dogan copper deposit (south of Shahroud): copper-molybdenum porphyry mineralization in the Toroud-Chah Shirin magmatic arc. J. Econ. Geol.

Fard, M., Rastad, E., Ghaderi, M., 2006. Epithermal gold and base metal mineralization at Gandy deposit, north of Central Iran and the role of rhyolitic intrusions. J. Sci. Islamic Republic of Iran 17 (4), 327–335.

Gantz, J., Reinsel, D., 2012. The digital universe in 2020: Big data, bigger digital shadows, and biggest growth in the far east. IDC iView: IDC Anal. Future 2007 (2012), 1–16.

Geological map of Toroud, 1:250,000 Series, 1978. Geological Survey of Iran (GSI).

Grigorian, S.V., Liakhovich, T.T., Getmansky, I.I., Ziaii, M., 1999a. Trace elements in minerals as a criterion of geochemical anomaly estimations. J. Sci. Technol. 1, 22–26. In Russian with English abstract.

Grigorian, S.V., Liakhovich, T.T., Getmansky, I.I., Ziaii, M., 1999b. Geochemical spectrum of minerals as a criterion of gold ores type identification. J. Sci. Technol. 3, 5–8. In Russian with English abstract.

Grigorian, S.V., Liakhovich, T.T., 2000. Guidelines for the assessment of geochemical anomalies by trace elements in minerals (on the example of gold deposits). IMGRE RAS. In Russian.

Grigorian, S.V., 1985. Secondary Lithochemical Haloes in Prospecting for Hidden Mineralization. Nedra Publishing House, Moscow. 176 pp. (in Russian).

Grigorian, S.V., 1992. Mining Geochemistry. Nauka, Moscow (In Russian).

Hassanzadeh, J., Ghazi, A.M., Axen, G. and Guest, B., 2002. Oligo-Miocene mafic-alkaline magmatism in north and northwest of Iran: Evidence for the separation of the Alborz from the Urumieh-Dokhtar magmatic arc. In Geological Society of America Abstracts with Programs (Vol. 34, No. 6, p. 331).

Heidari, S.M., Afzal, P., Ghaderi, M., Sadeghi, B., 2021. Detection of mineralization stages using zonality and multifractal modeling based on geological and geochemical data in the Au-(Cu) intrusion-related Gouzal-Bolagh deposit, NW Iran. Ore Geol. Rev. 139, 104561.

Hu, H., Wen, Y., Chua, T.S., Li, X., 2014. Toward scalable systems for big data analytics: A technology tutorial. IEEE Access 2, 652–687.

Hushmandzadeh, A.R., Alavi Naini, M. and Haghipour, A.A., 1978. Evolution of geological phenomenon in Troud area: Geological Survey of Iran (No. H5, p.136). Report. (In Persian).
Keynejad, A., Pourkermani, M., Arian, M., Saeedi, A., Lotfi, M., 2011. Dynamic analysis of fractures in north of Torud-Moalleman area, south of Damghan. Geosciences 20 (78), 3–16 in Persian with English abstract.
Kitchin, R., McArdle, G., 2016. What makes Big Data, Big Data? Exploring the ontological characteristics of 26 datasets. Big Data Soc. 3 (1), 1–10.
Kuzmenkova, N.V., Vorobyova, T.A., 2015. Landscape-geochemical mapping of the North-West of Kola Peninsula. J. Geochem. Explor. 154, 194–199.
Laney, D., 2001. 3D data management: Controlling data volume, velocity and variety. META Group Res. Note 6 (70), 1.
Li, S., Chen, J., Xiang, J., 2020. Applications of deep convolutional neural networks in prospecting prediction based on two-dimensional geological big data. Neural Comput. Appl. 32 (7), 2037–2053.
Li, S., Chen, J., Liu, C., 2022. Overview on the Development of Intelligent Methods for Mineral Resource Prediction under the Background of Geological Big Data. Minerals 12 (5), 616.
Liu, P., Di, L., Du, Q., Wang, L., 2018. Remote sensing big data: Theory, methods and applications. Remote Sens. (Basel) 10 (5), 711.
Ma, Y., Wu, H., Wang, L., Huang, B., Ranjan, R., Zomaya, A., Jie, W., 2015. Remote sensing big data computing: Challenges and opportunities. Futur. Gener. Comput. Syst. 51, 47–60.
Macheyeki, A.S., Kafumu, D.P., Li, X. and Yuan, F., 2020. Applied Geochemistry: Advances in Mineral Exploration Techniques. Elsevier. (Translate to Persian: Yazdi, A. and Dabiri, R., 2021. Islamic Azad University Scientific and Academic Publishing, Mashhad Branch, Iran).
Ministry of Mines and Metals of Iran, 1996. Explanatory text of geochemical map of Moaleman (6960).
Mohamed, A., Najafabadi, M.K., Wah, Y.B., Zaman, E.A.K., Maskat, R., 2020. The state of the art and taxonomy of big data analytics: view from new big data framework. Artif. Intell. Rev. 53 (2), 989–1037.
Nti, I.K., Quarcoo, J.A., Aning, J., Fosu, G.K., 2022. A mini-review of machine learning in big data analytics: Applications, challenges, and prospects. Big Data Mining Anal. 5 (2), 81–97.
Perelman, A.I., 1975. Landscape Geochemistry. Publishing Vysshaya shkola, Moscow (In Russian).
Philip, R., 2011. Big data analytics. TDWI Res. Fourth Quarter 6.
Qiu, J., Wu, Q., Ding, G., Xu, Y., Feng, S., 2016. A survey of machine learning for big data processing. EURASIP J. Adv. Signal Process. 2016, 1–16.
Rezaeeshahzadeh, Z., Bouzari, S., Badakhshanmomtaz, G., 2012. Relation of gold mineralization with tectonic and fault structures of gandiarea (south of Damghan). J. Earth 6 (22), 107–114.
Safari, S., Ziaii, M., 2019. Singularity of zonality, the indicator for quantitative evaluation of anomalies in mining geochemistry, Case study: Kerver. J. Mining Eng. 14 (42), 76–91.
Safari, S., Ziaii, M., 2020. Analysis of Data in Kerver Area for Detection of Blind Mineralization Using Singularity Method. J. Anal. Numer. Methods Mining Eng. 9 (21), 21–31.
Safari, S., Ziaii, M., Ghoorchi, M., 2016. Integration of singularity and zonality methods for prospectivity map of blind mineralization. Int. J. Mining Geo-Eng. 50 (2), 189–194.
Safari, S., Ziaii, M., Ghoorchi, M., Sadeghi, M., 2018. Application of concentration gradient coefficients in mining geochemistry: A comparison of copper mineralization in Iran and Canada. J. Mining Environ. 9 (1), 277–292.
Safonov, Y.G., 1997. Hydrothermal gold deposits: distribution, geological genetic types, and productivity of ore-forming systems. Geol. Ore Deposits 39 (1), 20–32.
Shamanian, G.H., Hedenquist, J.W., Hattori, K.H., Hassanzadeh, J., 2004. The Gandy and Abolhassani epithermal prospects in the Alborz magmatic arc, Semnan province, Northern Iran. Econ. Geol. 99 (4), 691–712.
Sochevanov, N. N., (1961). Method of sampling of underground workings and surface in search of ore bodies and deposits on the primary dispersion halos. B. Sat: Problems. Techniques for testing of ore deposits in the exploration and exploitation. Gosgeoltekhizdat (in Russian).
Solovov, A.P. and Garanin, A.V., 1972. Geochemical spectra of anomalies and identification of differences between similar objects. Nauka. (In Russian).
Solovov, A.P., Garanin, A.V., 1968. Geochemical spectra of anomalies and discriminant analysis. in: Lithochemical search for deposits by their supergene aureoles and dispersion flows. (In Russian).
Solovov, A.P., 1987. Geochemical Prospecting for Mineral Deposits (Kuznetsov, V.V., Trans.) (Englsih Edition). Mir, Moscow.
Sun, A.Y., Scanlon, B.R., 2019. How can Big Data and machine learning benefit environment and water management: a survey of methods, applications, and future directions. Environ. Res. Lett. 14 (7), 073001.
TaleFazel, E., Mehrabi, B., GhasemiSiani, M., 2019. Epithermal systems of the Torud-Chah Shirin district, northern Iran: Ore-fluid evolution and geodynamic setting. Ore Geol. Rev. 109, 253–275.
Tewari, S., Dwivedi, U.D., 2019. Ensemble-based big data analytics of lithofacies for automatic development of petroleum reservoirs. Comput. Ind. Eng. 128, 937–947.
Timkin, T., Abedini, M., Ziaii, M., Ghasemi, M.R., 2022. Geochemical and Hydrothermal Alteration Patterns of the Abrisham-Rud Porphyry Copper District, Semnan Province, Iran. Minerals 12 (1), 103.
Tsai, C.W., Lai, C.F., Chao, H.C., Vasilakos, A.V., 2015. Big data analytics: a survey. J. Big data 2 (1), 1–32.
Veselovskii, A.V., Meshcheryakova, V.B., 2007. The data bank on the geology of mineral resources. Autom. Doc. Math. Ling. 41 (1), 11–16.
Xiong, Y., Zuo, R., Carranza, E.J.M., 2018. Mapping mineral prospectivity through big data analytics and a deep learning algorithm. Ore Geol. Rev. 102, 811–817.
Xu, H., Zhang, C., 2023. Development and applications of GIS-based spatial analysis in environmental geochemistry in the big data era. Environ. Geochem. Health 45 (4), 1079–1090.
Yu, P., Chen, J., Chai, F., Zheng, X., Yu, M., Xu, B., 2015. Research on model-driven quantitative prediction and evaluation of mineral resources based on geological big data concept. Geol. Bull. China 34 (7), 1333–1343.
Zakir, J., Seymour, T., Berg, K., 2015. Big data analytics. Issues Inform. Syst. 16 (2).
Zhang, S.E., Nwaila, G.T., Bourdeau, J.E., Ghorbani, Y., Carranza, E.J.M., 2023. Deriving big geochemical data from high-resolution remote sensing data via machine learning: application to a tailing storage facility in the Witwatersrand goldfields. Artific. Intell. Geosci. 4, 9–21.
Zhao, P.D., 2015. Digital mineral exploration and quantitative evaluation in the big data age. Geol. Bull. China 34 (7), 1255–1259.
Zheng, X., Li, J.C., Wang, X., Liang, W.J., 2015. Construction of the national geological information service system in the age of big data. Geol. Bull. China 34 (7), 1316–1322.
Ziaii, M., Abedi, A., Ziaei, M., 2009a. Geochemical and mineralogical pattern recognition and modeling with a Bayesian approach to hydrothermal gold deposits. Appl. Geochem. 24 (6), 1142–1146.
Ziaii, M., Poyan, A., Ziaei, M., 2009b. A computational optimized extended model for mineral potential mapping based on WofE method. Am. J. Appl. Sci. 6 (2), 200–203.
Ziaii, M., Abedi, A., Ziaei, M., Kamkar Rouhani, A., Zendahdel, A., 2010. GIS modelling for Au-Pb-Zn potential mapping in Torud-Chah Shirin area-Iran. J. Mining Environ. 1 (1).
Ziaii, M., Carranza, E.J.M., Ziaei, M., 2011. Application of geochemical zonality coefficients in mineral prospectivity mapping. Comput. Geosci. 37 (12), 1935–1945.
Ziaii, M., Doulati Ardejani, F., Ziaei, M., Soleymani, A.A., 2012. Neuro-fuzzy modeling based genetic algorithms for identification of geochemical anomalies in mining geochemistry. Appl. Geochem. 27 (3), 663–676.
Ziaii, M., Abedi, A. and Ziaii, M., 2007, September. Prediction of hidden ore bodies by new integrated computational model in marginal Lut region in east of Iran. In Proc. Exploration 07: Fifth Decennial International Conference Mineral Exploration, Toronto, Canada, (Vol. 7, pp.957-961).
Ziaii, M., Safari, S., Timkin, T., Voroshilov, V., Yakich, T., 2019. Identification of geochemical anomalies of the porphyry–Cu deposits using concentration gradient modelling: A case study, Jebal-Barez area, Iran. J. Geochem. Explor. 199, 16–30.
Ziaii, M., 1999. PhD Thesis: Method of rational mineralogical and geochemical sampling of gold ore occurrences. Russian Academy of Science (IGEM RAN), Moscow. (In Russian).
Zuo, R., Xiong, Y., 2020. Geodata science and geochemical mapping. J. Geochem. Explor. 209, 106.
Zuo, R., Carranza, E.J.M., Wang, J., 2016. Spatial analysis and visualization of exploration geochemical data. Earth Sci. Rev. 158, 9–18.
Zuo, R., Xiong, Y., 2018. Big data analytics of identifying geochemical anomalies supported by machine learning methods. Nat. Resour. Res. 27, 5–13.
Zuo, R., Xiong, Y., Wang, J., Carranza, E.J.M., 2019. Deep learning and its application in geochemical mapping. Earth Sci. Rev. 192, 1–14.